Research Square

Preprints are preliminary reports that have not undergone peer review.
They should not be considered conclusive, used to inform clinical practice,
or referenced by the media as validated information.

Comparative Study of Atmospheric and Submerged AWJM Performance on Nimonic-90 Superalloy: Depth of Penetration Analysis and Hybrid Cohort Intelligence Modeling

Dilip Maruthi G

gdm.mech@bmsce.ac.in

BMS College Of Engineering

Sudhakar C Jambagi

National Institute of Technology Karnataka

Article

Keywords: Abrasive Water Jet Machining, Submerged Abrasive Water Jet Machining, Cohort intelligence, Depth of penetration, Hybrid algorithm, Nimonic 90

Posted Date: March 23rd, 2026

DOI: https://doi.org/10.21203/rs.3.rs-8993328/v1

License: This work is licensed under a Creative Commons Attribution 4.0 International License.
Read Full License

Additional Declarations: No competing interests reported.

Comparative Study of Atmospheric and Submerged AWJM Performance on Nimonic-90 Superalloy: Depth of Penetration Analysis and Hybrid Cohort Intelligence Modeling

Dilip Maruthi G[1,2*] and Sudhakar C Jambagi[2]

[1]Department of Mechanical Engineering,B.M.S. College of Engineering, Bull temple road, Bengaluru, 560019, Karnataka, India.
[2*]Department of Mechanical Engineering, National Institute of Technology Karnataka, Srinivasnagar, Surathkal, 575025, Karnataka, India.

*Corresponding author(s). E-mail(s): gdm.mech@bmsce.ac.in;
Contributing authors: sudhakar@nitk.edu.in;

Abstract

This research investigates the performance of Abrasive Water Jet Machining (AWJM) on the Nimonic 90 superalloy, specifically focusing on the influence of operational environment, atmospheric versus submerged, on the Depth of Penetration (DOP) and resulting surface finish. Experimental analysis revealed that atmospheric machining resulted in a higher maximum DOP of $\mathbf{37.46 \pm 3.01}$ mm (at **275** MPa), while the submerged condition consistently produced a smoother surface finish ($\boldsymbol{R_a}$ range: **1.91** to **4.45** $\boldsymbol{\mu}$**m**) due to the water's damping effect. Traverse Speed (TS) was identified as the most dominant control factor for DOP ($\boldsymbol{\Delta = 6.36}$), where increasing TS by $\sim$ **45%** caused a considerable reduction in penetration. For predictive modeling, a novel hybrid algorithm integrating Cohort Intelligence (CI) with linear regression was developed, exhibiting exceptional accuracy, particularly under submerged conditions, with a Pearson correlation coefficient ($\mathbf{R^2}$) of **0.9863** and a low MSE (**MSE**) of **0.750**. This research validates SAWJM as a robust, low-noise alternative for machining Nimonic 90 when surface integrity is prioritized over maximum depth, and it offers a highly accurate hybrid model for process optimization

Keywords: Abrasive Water Jet Machining, Submerged Abrasive Water Jet Machining, Cohort intelligence, Depth of penetration, Hybrid algorithm, Nimonic 90

1 Introduction

Nimonic 90 is a nickel-based superalloy extensively used in the nuclear, marine, and aerospace industries. Nickel alloys are used for approximately 50% of the components in aerospace engines[1]. However, Nimonic 90 poses significant challenges in machining, especially under dry conditions, owing to its strong chemical reactivity and insufficient thermal conductivity, which lead to material adhesion and accelerated tool wear[2–4]. Extensive research has shown that the friction encountered during the cutting process induces elevated temperatures, thereby accelerating the wear of cutting tools [5, 6]. Conventional techniques, such as drilling and milling, also struggle to achieve an optimal surface finish because of high cutting forces and energy demands. [7]Lower velocities aggravate tool wear, whereas higher speeds weaken the alloy, reducing cutting energy [8, 9]. However, the conventional machining of Nimonic 90 remains challenging. Abrasive Water Jet Machining (AWJM) is recommended to overcome these difficulties.

AWJM uses high-pressure water (200–400 MPa) and abrasives to produce a high-velocity jet for the precise cutting of various materials and has been considered a pioneering technology since 1979 [10].AWJM's non-thermal cutting is ideal for heat-sensitive materials as it preserves their properties. It supports sustainable manufacturing by utilizing water and eco-friendly abrasives such as garnet without generating harmful waste or emissions [11]. The quality of the AWJM processed workpiece is influenced by the traverse speed (TS), abrasive flow rate (AFR), and water pressure (WP). The WP provides cutting energy, AFR affects the surface quality and removal rate, and TS determines the cutting depth and precision. Optimizing the impact angle and standoff distance is essential for effective machining [11, 12]. AWJM removes material through erosion by high-velocity abrasive particles that impact the target surface [13]. The mechanism varies according to the material type: brittle materials are primarily removed through cracking, whereas ductile materials, such as metals, undergo micro cutting, plastic deformation, and chipping [14]. AWJM inherently involves dynamic surface changes owing to repeated abrasive impacts, which significantly influence erosion and surface finish [15]. Finite element analysis revealed that repeated interactions with abrasive particles continuously altered the surface, thereby affecting the cutting accuracy and removal efficiencies. AWJM is complex yet effective for machining difficult-to-cut materials because of its dynamic impact-response relationship[16].AWJM is commonly used for alloys such as Inconel, Ti-6Al-4V, and Nimonic 90, among others. The critical factors include WP, TS, AFR, particle size, standoff distance, nozzle diameter, and mixing tube length [17, 18].Studies have shown that a higher WP enhances smooth cutting zones and DOP, whereas a higher TS increases DOP but worsens surface quality. Larger abrasive particles can increase the scratches in machined surface also increases the roughness [18]. Studies on nickel-based super alloys have shown that combining optimal water pressure (WP) with a moderate traverse speed (TS) improves kerf geometry and reduces surface imperfections [19]. Traditional AWJM face challenges such as uneven material removal, rapid nozzle wear, and difficulties in maintaining kerf geometry in complex materials. For high precision, process control becomes challenging, often requiring adaptive or hybrid approaches. The Submerged Abrasive Water Jet

Machining(SAWJM) enhances stability, reduces splashing, and boosts precision by submerging the nozzle and work piece to specific depths. Ibrahim et al. (2020) reported a noise reduction from 108.8 dB in atmospheric AWJM to 86.1 dB when submerged owing to water damping and debris suppression. This setup also maintains surface smoothness by preventing damage caused by air debris [20]. James et al. found that the SOD and abrasive grit size significantly affected the cavity shape when cutting CFRP and Ti. A larger SOD enlarges the cavities owing to jet spreading, but submersion improves precision. Smaller abrasives create larger holes because they encounter flow issues. The SAWJM surpasses the AWJM in terms of dimensional precision and kerf-angle control[20, 21].

Accurate measurements of the Depth of Penetration (DOP) are essential for evaluating the AWJM performance. Yuvaraj et al. determined the penetration depth using a dial gauge to measure the surface cut length and identified the optimal conditions as a water pressure of 300 MPa, traverse speed of 120 mm/min, abrasive flow rate of 360 g/min, and standoff distance of 1 mm[22]. Zeng et al. introduced a needle insertion method after machining to measure multiple depths within a single cut. Another precise technique utilizes a profile projector to measure the cut length (L) by passing light through a trapezoidal specimen cut by AWJM, which is then correlated with the DOP[23, 24]. The machining results are influenced by component geometry and accuracy requirements. Adjustments to TS, AFR, WP, and SOD are crucial. A higher TS increased the speed but roughened the surface. Lower SOD, higher WP, and reduced AFR resulted in faster and smoother cutting. Machine Learning and genetic algorithms have simplified these decisions [25–27].

Machine Learning (ML) is playing an increasingly important role in predicting machining parameters. Jagadish et al. developed a smart system using subtractive clustering and a Takagi-Sugeno-Kang (TSK) fuzzy model to accurately predict surface roughness (Ra) in AWJM of green composites, based on Taguchi L27 experimental data and advanced soft computing techniques [28]. In addition, optimization algorithms such as teaching–learning–based optimization [29], Symbiotic Organism Search [30], and Collective Intelligence [31] have been applied to enhance the machining processes. Notably, the Multi-Cohort Intelligence (Multi-CI) algorithm has demonstrated superior performance in Ra and the taper angle in the AWJM and has been validated in manufacturing settings [32], outperforming traditional methods such as the Genetic Algorithm (GA), Simulated Annealing (SA), and Particle Swarm Optimization (PSO) [33]. Moreover, hybrid models combining minimizing optimization generalized linear regression with genetic algorithms have been proposed for the precise prediction of hot-rolling width deviation, leveraging the ability of linear regression to model the relationships between process variables and continuous outputs [34]. This study aimed to predict and optimize the DOP of Nimonic 90 using AWJM and SAWJM. A novel hybrid modeling framework integrating linear regression with cohort intelligence was proposed to improve prediction accuracy, an approach that has not been previously reported for this application. To the authors' knowledge, no prior experimental studies have systematically evaluated DOP under both AWJM and SAWJM conditions or examined the influence of submerged environments. These gaps were addressed through a combined experimental and computational approach. The proposed model

is applicable within the experimentally investigated parameter ranges, and predictions outside this domain may exhibit reduced accuracy, as extrapolation behavior was not validated. Extending the model's applicability beyond the current parameter space will require additional experimental validation.

2 Material selection and preparation

A Nimonic 90 block of dimensions 350 mm × 120 mm × 40 mm was used in this study. Titanium and aluminum enhance the Nimonic-90 alloy, making it highly ductile at temperatures up to 920 °C, age-hardened, and creep-resistant. Its high chromium content provides strong resistance to oxidation, corrosion, and heat. Nimonic-90 was selected for its unique composition Shown in Table 1 and challenging machinability using conventional methods.

Table 1 Chemical composition of the material (wt.%).

Element	C	Si	Cu	Fe	Mn	Cr	Ti
Composition	0.089	0.37	0.118	1.09	0.74	18.79	2.37
Element	Al	Co	B	S	Pb	Zr	Ni
Composition	1.28	17.36	0.02	0.015	0.002	0.15	57.58

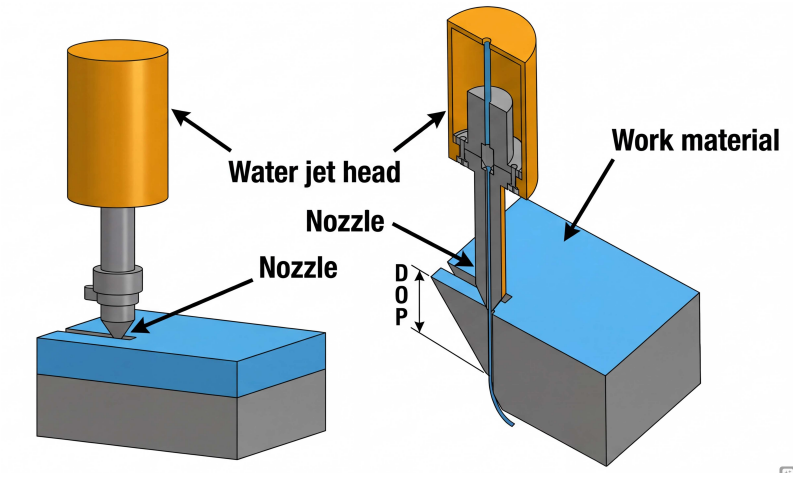


Fig. 1 (a) and (b) Schematic representation of the depth of penetration (DOP) into the trapezoidal workpiece.

Fig.1 a) and b) illustrate the trapezoidal workpieces fabricated using wire electro-discharge machining. This technique is renowned for its applicability in determining the DOP. The abrasive employed in this investigation was garnet, with the chemical

formula Fe3Al2Si3O12, as depicted in Fig.2 (a). The abrasive particle size was consistently maintained at an 80 mesh specification during the machining process. The particles were characterized using scanning electron microscopy (SEM) (TESCAN, VEGA3 LMU, CZECH REPUBLIC). The particles exhibited irregular shapes with sharp cutting edges, potentially resulting in microcutting and micropuffing phenomena during the machining operation [35]. The morphology and size of the abrasives are shown in Figures 2 b) and 2 c), accompanied by SEM and energy-dispersive X-ray analysis (EDAX).

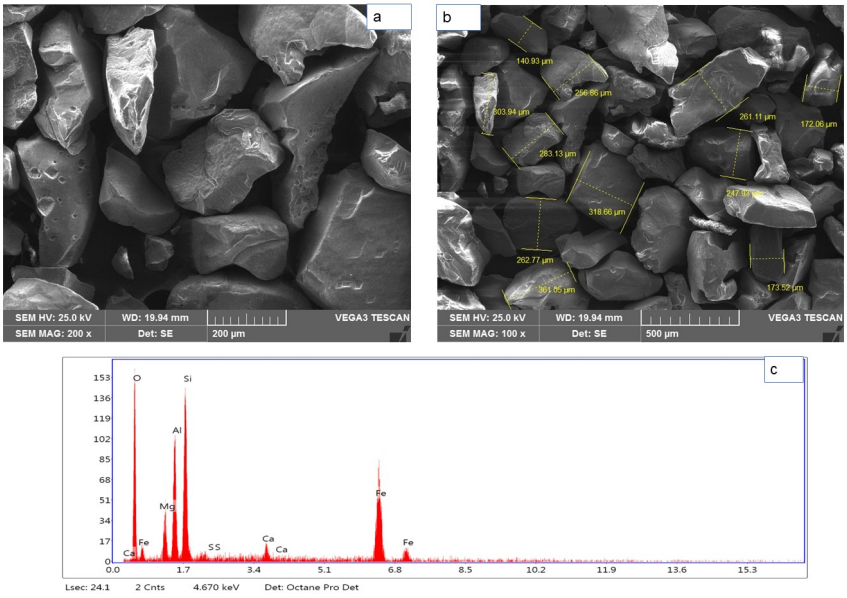


Fig. 2 a) and b) SEM morphology of garnet particles; c) EDAX of the garnet particles.

3 Experimentation and analysis

3.1 Experimentation

An AWJM center (OMAX, MAXIEM 1515, USA) with a pressure range of 100–345 MPa and a 30-hp pump were used in this study. The apparatus featured gravity-fed abrasives, pneumatically controlled movements (1575 mm × 1575 mm × 150 mm), and a transverse speed (TS) range of 1–8000 mm/min. Using a 0.35 mm sapphire orifice and 0.76 mm tungsten carbide nozzle, experiments were conducted under atmospheric and submerged conditions with a trapezoidal workpiece, as shown in Fig. 1. This study employed 80 mesh garnet particles were employed. This study focused on the DOP under various conditions. A three full factorial design with 27 trials was used

to examine the effect of parameters such as WP (225, 250, 275 MPa), TS (50, 100, 150 mm/min), AFR (200, 300, 400 g/min), and standoff distances (1, 2, 3 mm) under both conditions, with submerged depths of 5, 10, and 15 mm considered as well. The selected pressure range was chosen to ensure stable jet formation, consistent abrasive entrainment, and safe operation of the experimental system; however, higher pressure regimes commonly reported for AWJM (300–400 MPa) were not explored, which may limit the direct assessment of cutting performance under extreme jet energy conditions, particularly for difficult-to-machine alloys such as Nimonic-90 [36],[37]. Parameters such as the mixing tube length (100 mm), nozzle diameter (0.35 mm), and impact angle (90°) were maintained constant during machining under both conditions.We chose fixed parameters—mixing tube length (100 mm), nozzle orifice diameter (0.41 mm), and impact angle (90°) following OMAX MAXIEM 1515 specifications, manufacturer advice, and AWJM studies for reliable jet stability, even abrasive mixing, and steady energy delivery. This standard setup (L/D ratio 100) minimizes jet divergence. The 90° angle rules out geometry effects, letting us pinpoint how pressure, flow rate, speed, and standoff distance affects the DOP also Quick pilot cuts confirmed consistent results before full runs. Keeping them constant avoided random noise in our data.An 80-mesh garnet abrasive was selected to ensure stable abrasive flow and repeatable cutting performance [38].A Taguchi L27 orthogonal array was employed to investigate the effects of four primary control parameters WP,TS, AFR, and SOD each at three levels. The Taguchi design was applied exclusively to these four factors, and the corresponding experimental levels are listed in Table 2. DOP was measured three times for each experimental condition and the average value was used to minimize measurement uncertainty. Submerged depth was not included as a factor in the Taguchi design; instead, submerged depths of 5, 10, and 15 mm were examined through separate supplementary experiments under submerged conditions to evaluate their comparative influence on machining performance. Accordingly, submerged depth was excluded from the Taguchi-based ANOVA and optimization analysis to maintain consistency with the experimental design framework. The DOP was measured using a Vernier height gauge after AWJM machining under both atmospheric and submerged conditions. Fig. 3 shows the AWJM schematic. SEM was used to analyze the cut surface, and a 3D profilometer (NANOVEA, ST400, USA) was used to assess the surface quality for both conditions.

Table 2 Machining parameters and their levels for atmospheric and submerged conditions.

Factors	Level 1	Level 2	Level 3
Abrasive ater jet pressure (MPa)	225	250	275
Abrasive flow rate (g/min)	200	300	400
Traverse speed (mm/min)	50	100	150
SOD (mm)	1	2	3

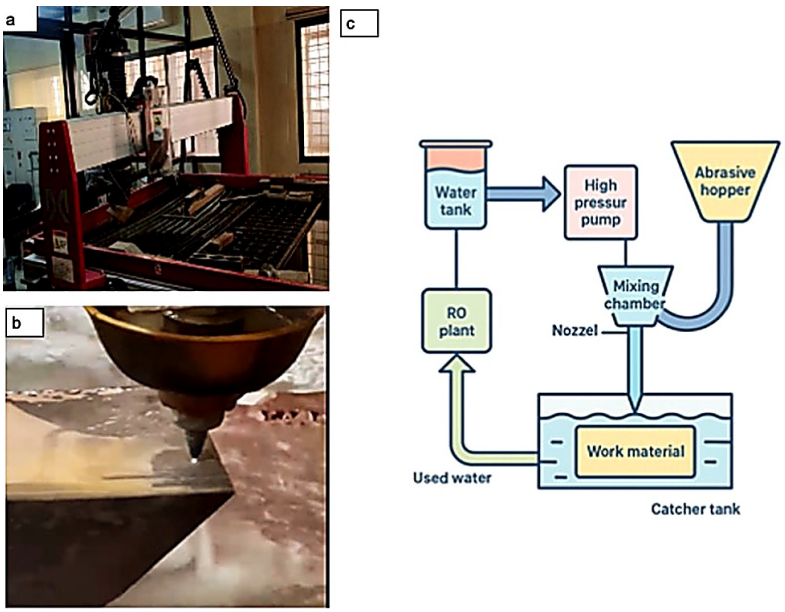


Fig. 3 Schematic representation of the Abrasive Water Jet Machine (OMAX 15150).

3.2 Cohort intelligence

The Cohort Intelligence (CI) algorithm is a socio-inspired optimization method rooted in group learning and problem-solving, similar to how students learn or athletes improve through observation. Unlike classic methods, such as particle swarm optimization (PSO) or ant colony optimization (ACO), which are based on natural behaviors, CI focuses on human social learning to solve complex problems [39]. The CI is a relatively novel optimization approach introduced by [39]. CI is a novel method inspired by cohorts working towards a common goal, in contrast to PSO or ACO, which emulate animal behavior optimization, as introduced by [39]. CI, which is based on human social learning, was used to determine the optimal parameters, focusing on collective knowledge rather than on individual data points. Unlike the instance-specific training of traditional machine learning, CI leverages the similarities among data groups to boost model performance and recognize patterns. It can enhance the AWJM process efficiency through cohort analyses and data aggregation. The analysis involved the cohort parameters WP, TS, AFR, and stand-off distance, defined by the DOE, with a population size of 100 and 100 iterations. Cohort candidates were randomly generated, similar to other population-based methods. The model performance was assessed using the mean square error (MSE) fitness function, as expressed in Equation (1).

$$MSE = 1/n \sum_{i=1}^{n} (Ytrue - Ypred)^2 \tag{1}$$

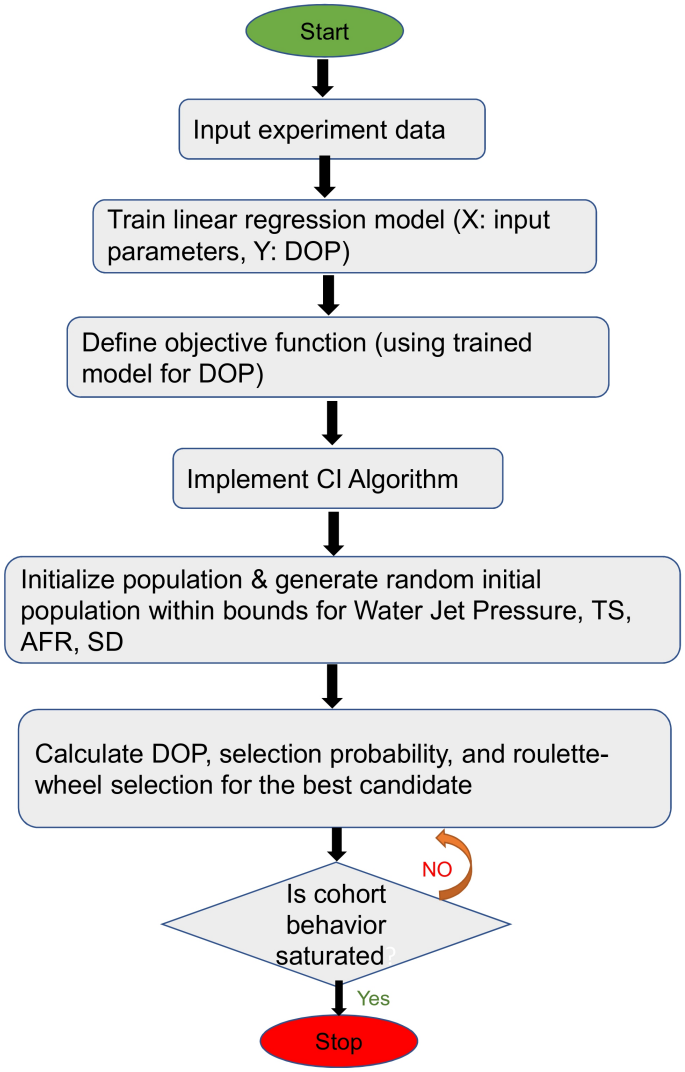


Fig. 4 Hybrid algorithm combining Cohort Intelligence and Linear Regression.

where n is the number of trials, Y true is the experimental value, and Y pred is the predicted value of the model. The probability of the selection behaviour of every associated candidate is calculated as follows in Equation(2)

$$P_i = \frac{\frac{1}{f(x_i)}}{\sum_{k=1}^{n} \frac{1}{f(x_k)}} \tag{2}$$

(Where Pi is the probability associated with each candidate, f (x) is the fitness value of the i-th candidate, evaluated MSE candidate, evaluated using the mean squared error (MSE) between and n is the number of trials.) where $\sum_{k=1}^{n} \frac{1}{f(x_k)}$ is the normalization factor, which ensures that the sum of the selection probabilities of all candidates equals unity, i.e.,

$$\sum_{i=1}^{n} P_i = 1. \tag{3}$$

Roulette Wheel Selection is widely used in genetic algorithms and other evolutionary methods, including Cohort CI, to find the optimal candidate. Each candidate autonomously chooses a behavior from the available options and iterates until the cohort achieves optimal behavior. If no significant improvement is observed, the behavior of each candidate represented by f (x) converges to the data. This study utilized Python code to optimize the parameters and enhance performance. The flow diagram is illustrated in Fig. 4.

3.3 Liner regression model

Linear regression predicts a continuous dependent variable using one or more independent variables, assuming a direct linear relationship. It evaluates how well the factors forecast the dependent variables. The model aims to determine the best line that represents the relationship between the dependent variable (DOP) and the independent variables. It is often expressed as an objective function, as shown in Eq. (3).

$$\text{DOP} = a \times \text{WP} + b \times \text{AFR} + c \times \text{TS} + d \times \text{SOD} + e \tag{4}$$

where

$$\begin{aligned} \text{DOP} &= \text{Depth of penetration (mm)}, \\ \text{WP} &= \text{Water jet pressure (MPa)}, \\ \text{AFR} &= \text{Abrasive flow rate (g/min)}, \\ \text{TS} &= \text{Traverse speed (mm/min)}, \\ \text{SOD} &= \text{Stand-off distance (mm)}, \\ a, b, c, d, e &= \text{Coefficients associated with the respective parameters.} \end{aligned}$$

Where:

- WP = Water Jet Pressure (MPa)
- AFR = Abrasive flow rate (g/min)
- TS = Traverse speed (mm/min)
- SOD = Stand-off distance (mm)

- DOP = Depth of penetration (mm)
- a, b, c, d, and e are the coefficients associated with each parameter

3.4 Hybrid CI–Linear Regression Model

The proposed hybrid modeling framework combines Cohort Intelligence (CI) and linear regression in a sequential and complementary manner to improve predictive performance. In this approach, CI is first used as a population-based search technique to explore the solution space and identify optimal or near-optimal combinations of input parameters. These optimized parameters are then used to build a linear regression model that captures the quantitative relationship between the inputs and the output response.[40],[41] The main advantage of this framework lies in the way the two methods are integrated. Rather than operating independently, CI acts as an intelligent pre-processing and optimization step that guides the regression model toward more informative parameter sets. This integration enhances both the accuracy and robustness of the predictions. By combining the exploratory capability of a meta-heuristic algorithm with the simplicity and interpret-ability of linear regression, the proposed hybrid approach is particularly effective for complex or high-dimensional modeling problems.[41],[42] Google Colab, a free cloud-based Jupyter notebook platform, is favoured for its ease of use and features like web-based Python execution without installation. It provides free access to the GPU and TPU to accelerate complex computations. This study used Python scripts for cohort and linear regression models to optimize and predict performance with the experimental dataset `.CSV`. NumPy is widely used for numerical computations because of its efficiency, particularly in data science and machine learning. The *sklearn.model* selection in scikit-learn is crucial for advancing machine learning models and offers tools for model selection, evaluation, cross-validation, parameter tuning and dataset partitioning. In this study, the dataset was split into training and testing subsets for comprehensive model evaluation. Our dataset is arranged with ≈27% designated for testing and ≈73% for training. This methodology allows the model to be trained on most of the data while assessing its performance on a separate subset and evaluating its generalization to new datasets. Both the cohort intelligence algorithm and linear regression model were implemented in Python using the scikit-learn library. The model library, MSE for the optimized values, and predicted DOP values were then determined.the final equation of the hibrid algorithm combined with ci and LR as shown below Equation(5)

$$\mathrm{DOP}_{\mathrm{CI–LR}} = \beta_0^* + \beta_1^* \,\mathrm{WP} + \beta_2^* \,\mathrm{AFR} + \beta_3^* \,\mathrm{TS} + \beta_4^* \,\mathrm{SOD} \tag{5}$$

where $\mathrm{DOP}_{\mathrm{CI–LR}}$ denotes the DOP predicted by the proposed hybrid model; β_0^* represents the optimized intercept term; β_1^*, β_2^*, β_3^*, and β_4^* are the optimized regression coefficients obtained through Cohort Intelligence; WP, AFR, TS, and SOD correspond to the Water Jet Pressure(MPa), abrasive flow rate (g/min), traverse speed (mm/min), and stand-off distance (mm), respectively.

4 Results and discussion

The experimental investigation of the AWJM of Nimonic 90 revealed marked differences in the DOP behavior across varying process parameters under atmospheric and submerged conditions. Atmospheric machining, characterized by a high WP and low TS, yielded the highest DOP, highlighting the significance of jet energy and duration of exposure in enhancing material removal efficiency. Although the overarching trends concerning parameter influence were consistent across both environments, submerged machining invariably resulted in slightly lower DOP values. This reduction was primarily attributed to energy dissipation and jet dispersion in the aqueous medium. Statistical analyses and optimization studies further corroborated these findings, demonstrating a substantial concordance between the experimental and predicted DOP values obtained using this model.

4.1 Effects of process parameters on the DOP in atmospheric conditions

Machining Nimonic 90 with AWJM under standard conditions yielded a maximum DOP of 37.46±3.01 mm using an SOD of 2 mm, WP of 275 MPa, AFR of 300 g/min, and TS of 50 mm/min. This peak DOP highlights WP's significant impact of WP, as increasing the WP boosts the DOP by enhancing the kinetic energy of the water jet and the velocity of the abrasive particles.[43, 44].Contrary to the influence of WP on DOP, an inverse relationship was observed for the TS. Specifically, an increase in WP was accompanied by a decrease in DOP at elevated TS. This phenomenon was recorded under conditions of a WP of 275 MPa, AFR of 300 g/min, and TS of 150 mm/min, where the resultant DOP measured 17±1.64 mm, indicating a $\approx$ 45% reduction owing to the increased TS, as the abrasive particles had insufficient time to erode the substrate effectively. Conversely, a higher DOP was observed with a reduced TS of 50 mm/min, which allowed sufficient time for material removal. A similar trend was observed in the machining of metal matrix composites (MMC) using AWJM. [45]. The DOP increased with the mass flow rate, which enhanced the abrasive particle interactions during cutting. The WP dominated the kinetic energy of the particles, and a higher WP increased the velocity and DOP. Experiments showed that raising WP from 225 MPa to 250 MPa, with an AFR of 200 g/min and TS of 100 mm/min, resulted in a $approx38\%$ increase in DOP, highlighting the importance of WP in enhancing DOP under high pressure.

4.2 Effects of process parameters on the DOP in submerged conditions

During machining of Nimonic-90 using AWJM at a WP of 275 MPa, AFR of 300 g/min, traverse speed of 50 mm/min, and a stand-off distance of 2 mm, a statistically significant difference in DOP was observed between atmospheric (37.46 ± 3.01 mm) and submerged conditions (35 ± 2.8 mm), corresponding to an approximate 6.6% reduction under submerged machining. Although the submerged environment introduces a hydrostatic pressure component as shown in Equation (4) order-of-magnitude

assessment shows that, for the submergence depths considered in this study (5–15 mm), the hydrostatic pressure is on the order of (10^2) Pa This value is several orders of magnitude smaller than the applied WP (10^8) and is therefore insufficient to dominantly govern the observed reduction in DOP. Consequently, hydrostatic pressure alone cannot explain the machining behavior under submerged conditions.

$$P_h = \rho g h \tag{6}$$

where

ρ = fluid density (kg/m^3),
g = acceleration due to gravity (m/s^2),
h = submersion depth (m).

This hydrostatic pressure P_h creates a stagnation effect that reduces the dynamic pressure of the Abrasive Water Jet (AWJM). Submersion also introduces viscous drag forces, expressed as:

$$F_d = \frac{1}{2}\rho \nu^2 C_d A \tag{7}$$

where

F_d drag force (N),
ρ fluid density (kg/m^3),
ν fluid velocity relative to the object (m/s),
C_d drag coefficient (dimensionless),
A cross-sectional area of the object exposed to flow (m^2).

The reduced DOP in submerged AWJM is instead primarily attributed to hydrodynamic effects arising from the interaction between the abrasive-laden jet and the surrounding water medium. These include viscous drag, turbulence generation, jet dispersion, and energy dissipation, which collectively reduce jet coherence, lower abrasive particle velocity, and promote momentum loss prior to impact with the workpiece. In this context, as shown in Equation (5) the drag force—governed by the drag coefficient C_d,A contributes to kinetic energy attenuation through turbulent energy transfer. Computational fluid dynamics studies have also demonstrated that submerged depth significantly influences DOP by modifying jet stability and abrasive transport behavior [46]. In the present experiments, increasing the submerged depth from 5 to 15 mm led to an increase in DOP, which is attributed to improved abrasive entrainment and reduced flow disturbance at greater immersion depths compared with the highly turbulent region observed at shallow submergence.

WP remained a critical parameter under both atmospheric and submerged conditions, with higher WP consistently producing greater DOP, as also reported for stainless steel and Inconel 715 [17, 35]. This behavior arises from the increased kinetic energy imparted to abrasive particles at higher pressures, a trend that persisted even under submerged conditions, as illustrated in Fig. 10(a) and (b). Traverse speed likewise played a dominant role, with lower TS values (e.g., 50 mm/min) yielding higher

DOP in both environments due to the increased interaction time between the jet and the work piece, as shown in Fig. 7.The submerged environment primarily influenced DOP through hydrodynamic damping, jet dispersion, and abrasive momentum loss, rather than through acoustic or pressure-related effects.

AFR also exerted a significant influence on DOP. Increasing AFR initially increased penetration under both environments by introducing more cutting particles into the jet; however, beyond an optimum range (300–400 g/min), further increases produced diminishing returns. This reduction is attributed to abrasive congestion, particle–particle collisions, and the formation of water–solid interaction layers within the mixing chamber, all of which reduce the specific kinetic energy of the abrasives. As a result, only marginal increases (approximately 1 mm) in DOP were observed at higher AFR levels, as shown in Fig. 7(c).From a modeling perspective, the hybrid Cohort Intelligence–Linear Regression framework demonstrated strong predictive capability for DOP under both atmospheric and submerged conditions. Under atmospheric machining, the model achieved a mean squared error of 1.010 with a Pearson correlation coefficient (($\mathbf{R^2 = 0.9811}$) while under submerged conditions the predictive accuracy improved further, yielding an MSE of 0.750 and an value of ($\mathbf{R^2 = 0.9863}$) The combination of high correlation and reduced error confirms the ability of the hybrid model to capture the complex inter dependencies between process parameters and machining performance [47]. However, since the proposed CI–linear regression model was not bench marked against other mainstream predictive approaches such as neural networks or evolutionary regression frameworks, claims regarding its comparative superiority remain limited. Future work will therefore focus on systematic bench marking to evaluate prediction accuracy, generalization capability, and computational efficiency.Optimization results obtained using the cohort intelligence algorithm indicated that the best DOP under atmospheric conditions was 30.514 ± 1.5 mm, achieved at WP = 230 MPa, AFR = 341 g/min, TS = 149 mm/min, and SOD = 2 mm. Under submerged conditions, the optimal DOP was approximately 30 mm, corresponding to WP = 262 MPa, AFR = 288 g/min, TS = 90 mm/min, and SOD = 1.5 mm. The close agreement between experimentally measured and optimized DOP values confirms the robustness of the hybrid modeling approach for prediction and optimization, as illustrated in Fig. 4.

4.3 Annova

The present study examined the effects of four process parameters, WP, AFR, TS, and SOD on DOP in AWJM under Atmospheric and Submerged conditions. The experiments were planned using a Taguchi L27 orthogonal array, and the signal-to-noise ratio (SNRA) and ANOVA were used for statistical analysis to determine the dominant factors. Interestingly, the ordering of the parameters was similar under both machining conditions, with TS being the most critical, followed by AFR, WP, and SOD. TS registered the greatest delta value ($\Delta = 6.36$) in atmospheric and submerged machining, reflecting its primary influence on DOP control. A reduced traverse speed allows the water jet containing the abrasive to spend more time removing material at each point, thereby increasing the DOP. This trend is well corroborated in the literature[48], which proves that a decrease in the traverse speed considerably improves

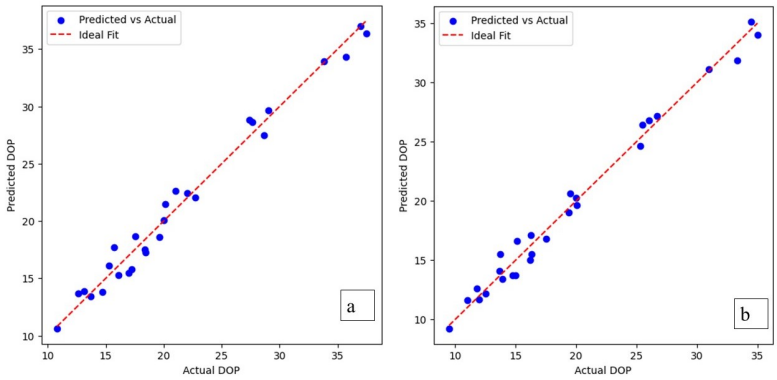


Fig. 5 Predicted DOP vs. True DOP under different conditions: (a) Atmospheric condition, (b) Submerged condition.

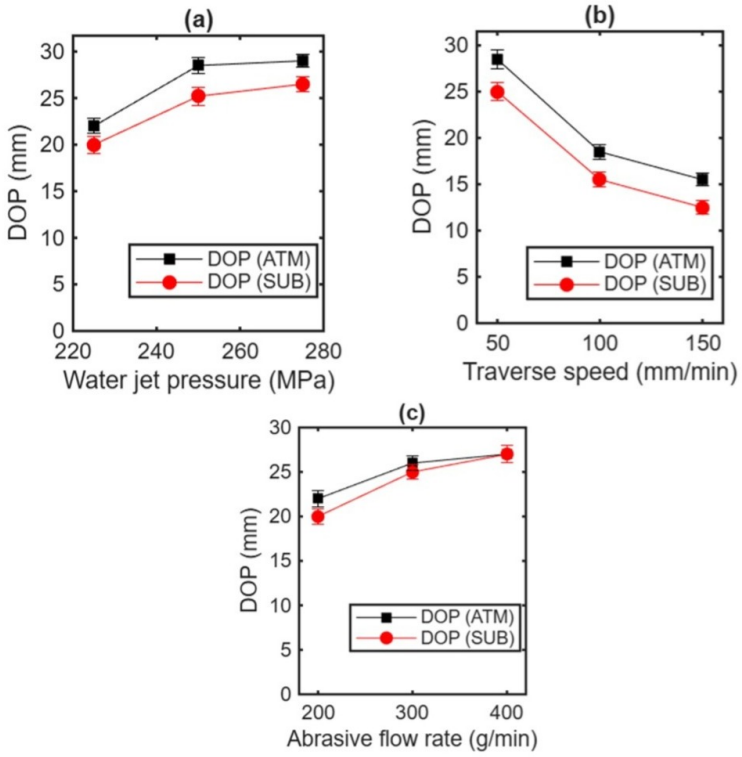


Fig. 6 Effect of key process parameters DOP under atmospheric and submerged AWJM conditions: (a) Influence of WP on DOP, (b) Influence of TS on DOP, (c) Influence of AFR on DOP.

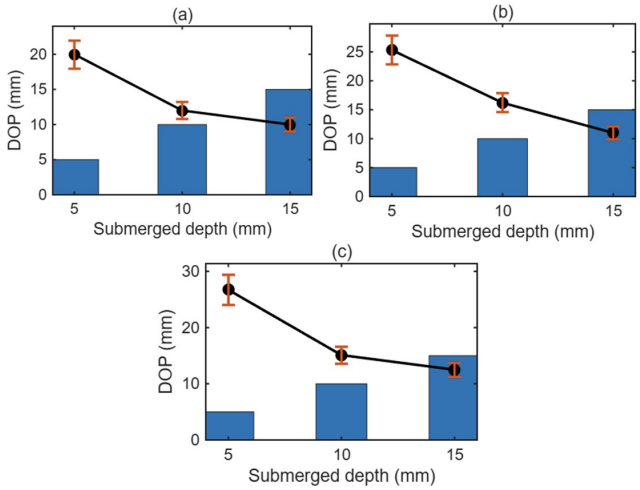


Fig. 7 Influence of submerged depth on DOP at different WP: (a) 225 MPa, (b) 250 MPa, (c) 275 MPa.

the energy transfer and erosion of the material in titanium alloys machined using AWJM. The effect of TS is further enhanced under submerged conditions, where the water medium diminishes the coherence and kinetic energy of the jet. Under such conditions, a reduced TS tends to reduce these losses, as was also found by [49]in their experiments with submerged castamide AWJM. AFR was the second most significant factor ($\Delta = 2.20$) in the model. An increased AFR causes more particles to impact the work surface, resulting in more effective material removal [50]. validated this behavior, showing that abrasive flow significantly promotes DOP in titanium alloys. Under submerged conditions, where the water medium tends to disperse the jet, an increased abrasive mass flow supports the cutting ability of the jet by promoting the momentum and density of particles. Although it was ranked third ($\Delta = 1.99$) for both conditions [51], it showed a comparatively lower practical impact in submerged cutting. In atmospheric machining, an increase in pressure results in a direct increase in jet velocity and energy, leading to deeper cuts. However, under submerged conditions, ambient water removes some of the jet energy in the form of turbulence and cavitation, thereby minimizing its effect on the work surface[52]. Similarly, analogous observations were reported under submerged conditions, where the AWJM could lose up to 35% of its cutting energy compared to the atmospheric AWJM under the same pressure conditions. SOD had the minimum impact ($\Delta = 0.35$) on the DOP in both cases, particularly within the narrow operational range of 1–2 mm. As the nozzle approaches the surface, the jet becomes coherent and efficient, making further SOD reduction irrelevant. This result supports the findings of the papers [16, 53], which determined that SOD becomes notably significant only when it is increased beyond the range of 3–4 mm, beyond which jet divergence intensifies. Under submerged conditions, the damping

characteristics of water further diminished the effect of minor variations in the SOD. A comparative analysis of the two environments revealed several key insights. TS emerged as the predominant parameter in both scenarios, and its significance was magnified in the SAWJM owing to the fluid damping effects[54]. AFR consistently plays an influential role and can be amplified in submerged settings to counteract energy losses. While advantageous under atmospheric conditions, WP exhibits diminishing returns under submerged conditions[55]. Investing additional funds in higher pressures for submerged applications is economically unfeasible. Finally, SOD can be regarded as a secondary consideration within narrow stand-off ranges and does not necessitate primary emphasis during process optimization. These findings are significant for the industrial implementation of AWJM, particularly when submerged machining is required, such as for noise control, reducing airborne dust, or cooling thermally sensitive materials. The analogous ranking of parameter influence across both conditions provides a reliable foundation for developing machining strategies that optimize both performance and cost efficiency. This is consistent with various studies [56], where optimizing TS and AFR constitutes the most effective approach to enhance DOP, especially under submerged conditions, where compensating for energy loss is imperative. The mean effect plots of DOP under atmospheric and submerged conditions are shown in Figures 6 and 7, respectively.

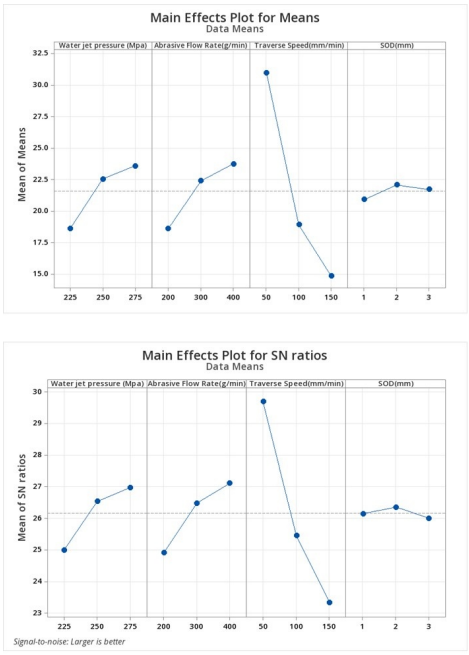


Fig. 8 Mean effect plots for DOP under atmospheric AWJM conditions.

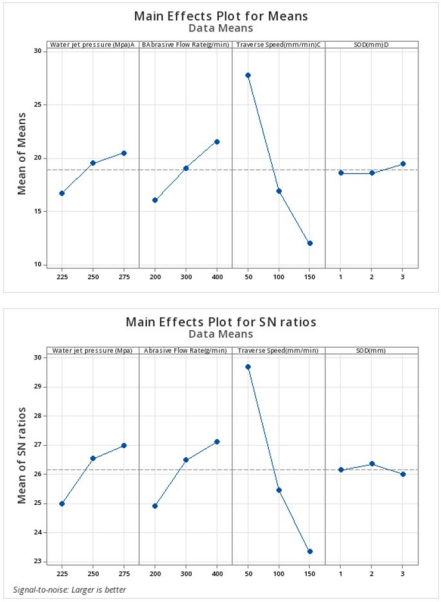


Fig. 9 Main effect plots for DOP under SAWJM conditions.

4.4 Microstructure characterization of machined surface

The sharp edges of the garnet particles, as shown in Fig. 2, strike the work piece owing to the high pressure of the water jet during the metal erosion removal process of an AWJM. As illustrated in Fig. 10, the cutting surface was not uniform but contained three distinct zones. The upper zone was smooth as well. In Nimonic 90, controlled erosion resulted in a smooth cutting zone with good surface quality. The second zone combined the rough and smooth areas. Once the cutting process begins, the high pressure of the jet stream causes the particles to batter the second surface, causing scratches in the second zone. The third zone is rough because the pressure and velocity decrease as the water jet impacts the first and second zones, causing the water stream to slant downward and create striations [24]. The 3D profilometer images in Fig. 12 show that the scratches have a distinct orientation. The TS, AFR, and WP are important factors that influence linear scratch formation during machining under atmospheric and submerged conditions [57]. In the current study, a high impact angle of 90 ° was used for the water jet. This results in maximum material removal precisely below the high-pressure water jet, and the abrasive particles follow a straight path until they lose their kinetic energy [58]. All the samples exhibited linear scratches in the direction of the water jet flow, as shown in Fig. 11. When the WP was 225MPa, abrasives were struck in the track at a high traverse speed of 150 mm/min. As shown in Fig.11(c), the water-jet pressure was insufficient to remove the abrasives. This result demonstrates that a high water-jet pressure is always preferred for the machining of Nimonic 90. The machined surface exhibited a large groove-shaped scratch during

submerged machining at a submerged depth of 5 mm when the WP was 250 MPa, TS was 150 mm/min, and AFR was 400 g/min, respectively, as shown in Figs. 11 (f) and (d). The abrasive grains are repeatedly impacted in the same place, and these abrasives are different in shape and size, showing overlapped scratches [59, 60] and groove scratches that correspond to the shape of the abrasive particle that is struck during machining[15]. This was also due to turbulence at a depth of 5 mm under submerged conditions. Microchipping occurs in the same sample, as shown in Fig.11(f), when abrasives strike the material and do not remove a lip and crater, leaving a micron-sized chip that matches the size of the abrasive particles[24, 43].

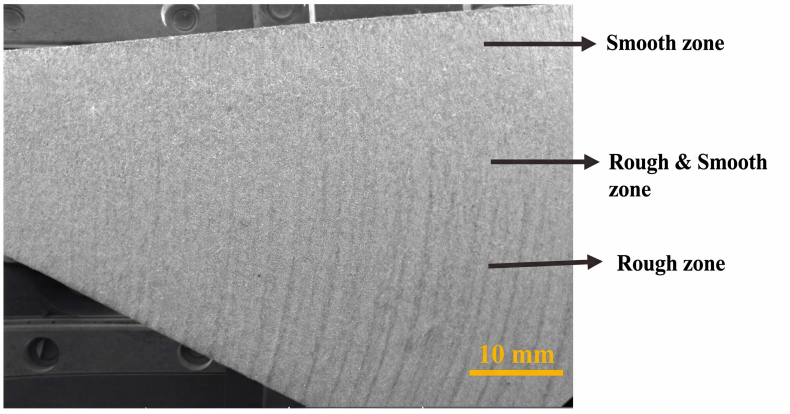


Fig. 10 Schematic representation of the AWJM Machined Micro structured image

4.5 Surface topography analyses of the machined surface

Three-dimensional profilometer maps (Fig.12(a–d)) provide a clear illustration of the influence of mechanical machining conditions and process parameters on the resulting surface texture in AWJM. In the context of atmospheric cutting at a WP of 225 MPa,AFR of 200 g/min, and a TS of 150 mm/min (Fig.12a), a concentrated grouping of red patches with peaks approximately ≈44µm above the mean plane is evident. Comparable "island-type" asperities emerge when moderate abrasive flow and traverse speed allow only partial overlap of subsequent jet footprints, thus creating uneroded zones between impacts[61].Increasing the WP to 27 MPa, adjusting the AFR to 300 g/min, and reducing the TS to 50 mm/min (Fig.12c) resulted in a predominantly green color field with occasional red occurrences. This indicates an expansion in the surface height range to ≈55 µm, while the texture becomes more uniform. According to the literature, a low traverse speed combined with high pressure prolongs the jet surface dwell time, leading to newly formed peaks being rapidly abraded, which flattens the micro-relief, albeit with an increase in the nominal Rz [53, 62]. also noticed the same synergy in precision finish research, wherein roughing conditions in conjunction with slow feed created smoother kerf walls at increased material removal rates[62, 63]. A

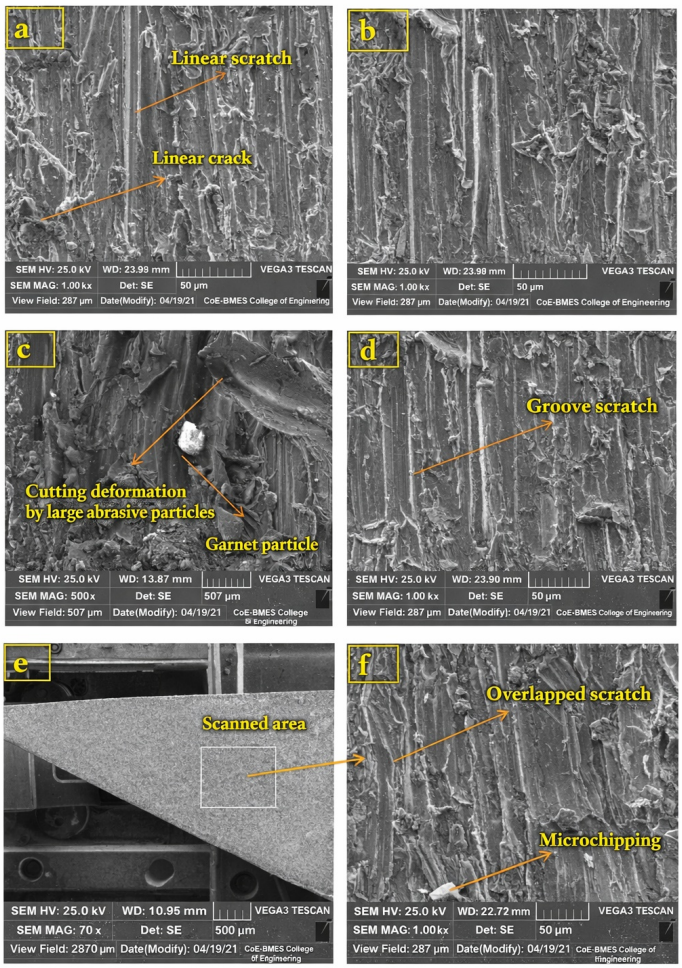


Fig. 11 Surface morphology of Nimonic-90 machined under atmospheric and submerged AWJM conditions: (a) Atmospheric condition at 275 MPa, 300 g/min, and 50 mm/min; (b) Submerged condition at 275 MPa, 200 g/min, and 100 mm/min with a submerged depth of 10 mm; (c) Atmospheric condition at 225 MPa, 200 g/min, and 150 mm/min; (d) Submerged condition at 250 MPa, 400 g/min, and 150 mm/min with a submerged depth of 5 mm; (e) Low-magnification view of machined surface at 275 MPa, 200 g/min, and 100 mm/min; (f) High-magnification view of the same surface.

distinctly different pattern was observed in the submerged regime (nozzle 5 mm submerged). At 250 MPa, AFR 400 g/min, and TS 150 mm/min (Fig.12 b), the water layer quenched the jet momentum, whereas the excess abrasive caused intense collisions between particles and splashback. The mottled surface has new red islands interspersed with a generally flat green background. AWJM experiments immersed in castamide and stainless steel reported a 20–30% increase in roughness when the abrasive feed was above an optimum because particle collision in the liquid phase reduced

particle energy prior to impact[64]. Maintaining pressure and speed invariance and reducing the abrasive flow by half to 200 g/min (Fig.12 (d) and (b)) produces fewer discernible red peaks and a more uniform green-yellow color scheme. discovered that moderate AFR is based on taking advantage of the water stabilization phenomenon, reducing Ra by as much as $\approx$ 25% with respect to excessive AFR in submerged conditions[65].Both submerged images have no directional striations and are thus consistent with the inference that shallow-immersion turbulence randomizes the particle paths. CFD simulations of SAWJM nozzles indicate intense vertical structures that disperse abrasives and eliminate machining direction signatures[46]. With an increase in the depth of the water column, the hydrostatic backpressure and viscous drag further reduced the jet velocity. Deep-sea modelling exercises predict a nearly quadratic reduction in particle kinetic energy with depth, leading to a detectable decrease in DOP, even at a constant pump pressure [46]. Our experiments (Fig. 7a–c) verified that raising submergence from 5 mm to 15 mm progressively lowered DOP, consistent with previous studies on cast iron and aluminum, in which the stand-off type hydrostatic resistance prevented DOP. Combining these surface observations with the Taguchi/ANOVA findings provides a consistent mechanism. Traverse speed continues to be the master lever for surface quality: lower feeds increase footprint overlap and smoothing in both media, consistent with Begić-Hajdarević et al., who associated increasing TS with greater roughness on aluminum plates [61]. The AFR has a dual function; it is positive in air if coupled with high pressure but negative when submerged after particle-to-particle damping takes over, similar to the results of Lima et al. for gemstone cutting[66] When the WP increases, erosion occurs wherever it is applied, but it provides decreasing returns in liquid baths, where the energy is lost to turbulence. Finally, the submergence depth behaved like a longer stand-off distance, with a hydrostatic resistance that systematically decreased the DOP. In practice, the findings suggest a moderate AFR, shallow submerged depth, and regulated TS for high-quality submerged machining; however, high pressure, copious abrasives, and very low TS remain optimal for achieving a higher DOP in air. Therefore, combined experimental and numerical evidence substantiates the assertion that the machining environment, along with an optimally balanced parameter set, determines whether productivity or surface finish is emphasized in the machining process. The surface roughness behavior is visualized using the 3D surface graphs in Fig.12. Under atmospheric conditions, Ra values varied from 1.31 to 31.4 µm, with the minimum roughness observed at 250 MPa, AFR 400 g/min, and TS 150 mm/min, and the maximum at 275 MPa, AFR 200 g/min, and TS 50 mm/min. The very high Ra at low TS and high pressure was due to the severe erosion and turbulent jet deflection. According to [67]. Increased energy concentration at low traverse speeds results in deeper craters and irregular erosion, enhancing surface roughness[68] In contrast, SAWJM had a lower and narrower roughness range of Ra from 1.91 to 4.45 µm. The optimum surface finish (Ra = $\approx$1.91 µm) was achieved at 275 MPa, an AFR of 200 g/min, and a TS of 100 mm/min, whereas the maximum value (Ra = $\approx$4.45 µm) was achieved at 225 MPa, an AFR of 300 g/min, and a TS of 50 mm/min. These findings reaffirm that the water medium is a damping environment for slowing down abrasive velocity fluctuations and splash-back, as substantiated by [69]

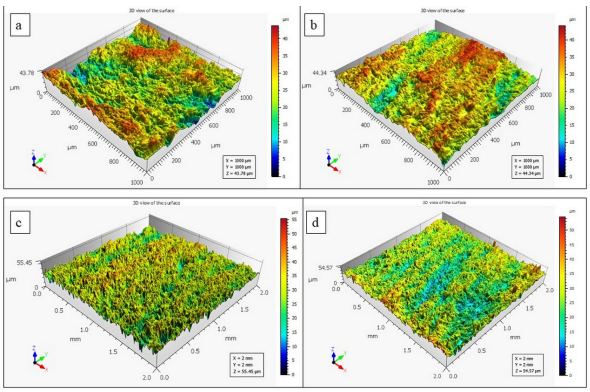


Fig. 12 3D surface images of machined surfaces under different conditions: (a) Atmospheric condition at 225 MPa, 200 g/min, and 150 mm/min; (b) Submerged condition at 250 MPa, 400 g/min, and 150 mm/min with a submerged depth of 5 mm; (c) Atmospheric condition at 275 MPa, 300 g/min, and 50 mm/min; (d) Submerged condition at 250 MPa, 200 g/min, and 150 mm/min with a submerged depth of 5 mm.

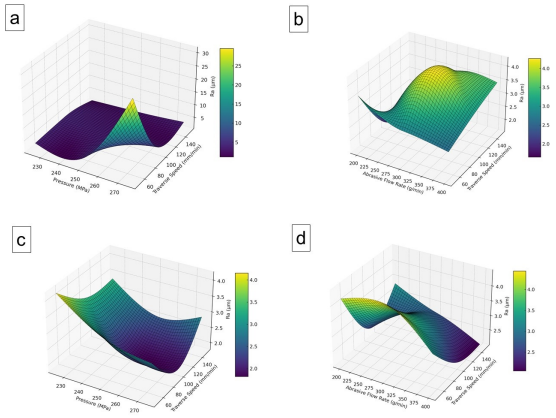


Fig. 13 Surface roughness of WJM sample

5 Conclusion

In this study, AWJM was performed on Nimonic 90 under two distinct conditions: atmospheric and submerged, with DOP as the primary measurement parameter. The experimental results were validated and scrutinized using a hybrid methodology that integrated cohort intelligence and linear regression analysis, supplemented by Analysis of Variance (ANOVA). Furthermore, Scanning Electron Microscopy (SEM) and a 3D profilometer were utilized to evaluate the surface topography and microstructural features, leading to the following conclusions.

- WP governs the overall cutting energy available during machining, with the maximum DOP of 37.46±3.01 mm obtained at 275 MPa. An increase in WP enhances the kinetic energy of the abrasive particles, thereby promoting deeper penetration.TS showed an inverse relationship with DOP; increasing TS reduced the interaction time between the jet and the work material, leading to a considerable reduction in penetration. A decrease of approximately 45% in DOP was observed when TS increased from 50 to 150 mm/min.
- Abrasive characteristics played an important role in determining surface integrity, particularly under submerged conditions. Microchipping and overlapping scratches were observed at a submerged depth of 5 mm due to intense turbulence, with scratch dimensions comparable to the abrasive particle size. At higher AFR , excessive abrasive loading led to partial nozzle blockage, jet de-focusing, and a reduction in cutting efficiency.
- The proposed hybrid model demonstrated strong predictive capability for DOP under both machining environments. Under atmospheric conditions, the model achieved a MSE of 1.010 with an R^2 value of 0.9811. Under submerged conditions, prediction accuracy improved further, yielding an MSE of 0.750 and an R^2 of 0.9863, indicating close agreement between experimental and predicted results.
- Atmospheric AWJM resulted in the highest surface roughness (Ra) of approximately 31.4 µm at 275 MPa, an AFR 200 g/min, and a TS of 50 mm/min due to severe erosion and jet turbulence. In contrast, a minimum Ra of approximately 1.31 µm was obtained at 250 MPa, an AFR of 400 g/min, and a TS of 150 mm/min, indicating that higher TS and AFR, combined with a balanced WP, improved surface finish while reducing DOP.
- Submerged AWJM consistently produced smoother surfaces, with Ra values ranging from 1.91 µm to 4.45 µm. The optimum surface finish (Ra = 1.91 µm) was achieved at 275 MPa, an AFR of 200 g/min, and a traverse speed of 100 mm/min. This confirms that moderate AFR and TS, together with the damping action of the water medium, enhance surface quality under submerged conditions.
- Taguchi analysis identified TS as the most statistically significant parameter influencing DOP in both atmospheric and submerged machining, exhibiting the highest delta value ($\Delta = 6.36$). AFR showed a secondary influence ($\Delta = 2.20$), followed by (WP, $\Delta = 1.99$) and SOD, $\Delta = 0.35$). These results indicate that TS and AFR provide the most effective control over DOP, particularly under submerged conditions where energy losses due to water damping are more pronounced.
- Based on the experimental observations and modeling results, SAWJM can be considered a viable alternative for machining Nimonic-90 when surface quality is prioritized. The variation in DOP between atmospheric and submerged conditions remained within approximately 20%, and further reductions in traverse speed can compensate for penetration loss. The effectiveness and reliability of the proposed hybrid modeling framework were successfully validated for both machining environments.

The results of this study should be viewed with an understanding of certain limitations. The experiments were conducted within a defined range of process parameters, and the findings have not yet been validated under large-scale industrial conditions.

Although submerged AWJM demonstrated clear benefits in terms of surface quality and noise reduction, its wider industrial use may be constrained by higher energy requirements and associated operating costs. Future studies will therefore focus on improving energy efficiency and carrying out detailed economic feasibility assessments to better support practical industrial implementation.

Declarations

Ethical Approval: This article does not contain any studies with human participants or animals performed by any of the authors.

Conflict of Interest: The authors declare that they have no conflict of interest.

Funding: No funding was received for conducting this study.

Author Contributions: [Dilip Maruthi G] – Conceptualization, Methodology, Investigation, Writing – original draft. [Sudhakar C Jambagi] – Supervision, Validation, Writing – review & editing.

Availability of Data and Materials: The data supporting the findings of this study are available from the corresponding author on reasonable request.

References

[1] Ezugwu, E., Bonney, J., Yamane, Y.: An overview of the machinability of aeroengine alloys. Journal of materials processing technology **134**(2), 233–253 (2003)

[2] Ghosh, S., Rao, P., al.: Performance evaluation of deep cryogenic processed carbide inserts during dry turning of nimonic 90 aerospace grade alloy. Tribology international **115**, 397–408 (2017)

[3] Patel, T., Khanna, N., Yadav, S., Shah, P., Sarikaya, M., Singh, D., Gupta, M.K., Kotkunde, N.: Machinability analysis of nickel-based superalloy nimonic 90: A comparison between wet and lco 2 as a cryogenic coolant. The International Journal of Advanced Manufacturing Technology **113**, 3613–3628 (2021)

[4] Roebuck, B., Loveday, M., Brooks, M.: Characterisation of nimonic 90 by the use of miniaturised multiproperty mechanical and physical tests. International journal of fatigue **30**(2), 345–351 (2008)

[5] Dhananchezian, M., Rajkumar, K.: Comparative study of cutting insert wear and roughness parameter (ra) while turning nimonic 90 and hastelloy c-276 by coated carbide inserts. Materials Today: Proceedings **22**, 1409–1416 (2020)

[6] Behera, B., Ghosh, S., Rao, P.: Wear behavior of pvd tin coated carbide inserts during machining of nimonic 90 and ti6al4v superalloys under dry and mql conditions. Ceramics International **42**(13), 14873–14885 (2016)

[7] Dahmus, J.B., Gutowski, T.G.: An environmental analysis of machining. In: ASME International Mechanical Engineering Congress and Exposition, vol. 47136, pp. 643–652 (2004)

[8] Khanna, N., Agrawal, C., Gupta, M.K., Song, Q., Singla, A.K.: Sustainability and machinability improvement of nimonic-90 using indigenously developed green hybrid machining technology. Journal of cleaner production **263**, 121402 (2020)

[9] Ghosh, S., Rao, P., al.: Specific cutting energy modeling for turning nickel-based nimonic 90 alloy under mql condition. International Journal of Mechanical Sciences **146**, 25–38 (2018)

[10] Wang, H., Yuan, R., Zhang, X., Zai, P., Deng, J.: Research progress in abrasive water jet processing technology. Micromachines **14**(8), 1526 (2023)

[11] Llanto, J.M., Tolouei-Rad, M., Vafadar, A., Aamir, M.: Recent progress trend on abrasive waterjet cutting of metallic materials: a review. Applied Sciences **11**(8), 3344 (2021)

[12] Natarajan, Y., Murugesan, P.K., Mohan, M., Khan, S.A.L.A.: Abrasive water jet machining process: A state of art of review. Journal of Manufacturing Processes

49, 271–322 (2020)

[13] Arola, D., Ramulu, M.: Material removal in abrasive waterjet machining of metals surface integrity and texture. Wear **210**(1-2), 50–58 (1997)

[14] Mieszala, M., Torrubia, P.L., Axinte, D.A., Schwiedrzik, J., Guo, Y., Mischler, S., Michler, J., Philippe, L.: Erosion mechanisms during abrasive waterjet machining: model microstructures and single particle experiments. Journal of Materials Processing Technology **247**, 92–102 (2017)

[15] Kumar, N., Shukla, M.: Finite element analysis of multi-particle impact on erosion in abrasive water jet machining of titanium alloy. Journal of Computational and Applied Mathematics **236**(18), 4600–4610 (2012)

[16] Salinas, L.C., Moussaoui, K., Hejjaji, A., Salem, M., Hor, A., Zitoune, R.: Influence of abrasive water jet parameters on the surface integrity of inconel 718. The International Journal of Advanced Manufacturing Technology **114**, 997–1009 (2021)

[17] Ay, M., Çaydaş, U., Hascalik, A.: Effect of traverse speed on abrasive waterjet machining of age hardened inconel 718 nickel-based superalloy. Materials and Manufacturing Processes **25**(10), 1160–1165 (2010)

[18] Fengchao, W., Kaining, Y., Nanzhe, X., Liucan, L., Chuwen, G.: Quantitative analysis on the surface topography of ti-6al-4v machined by abrasive suspension jet. The International Journal of Advanced Manufacturing Technology **112**, 323–332 (2021)

[19] Uthayakumar, M., Khan, M.A., Kumaran, S.T., Slota, A., Zajac, J.: Machinability of nickel-based superalloy by abrasive water jet machining. Materials and Manufacturing Processes **31**(13), 1733–1739 (2016)

[20] Haghbin, N., Spelt, J.K., Papini, M.: Abrasive waterjet micro-machining of channels in metals: comparison between machining in air and submerged in water. International journal of machine tools and manufacture **88**, 108–117 (2015)

[21] James, S., Mahajan, A.: Experimental study of machining of smart materials using submerged abrasive waterjet micromachining process. In: International Manufacturing Science and Engineering Conference, vol. 51388, pp. 004–03012 (2018). American Society of Mechanical Engineers

[22] Yuvaraj, N., Pradeep Kumar, M.: Multiresponse optimization of abrasive water jet cutting process parameters using topsis approach. Materials and Manufacturing Processes **30**(7), 882–889 (2015)

[23] Zeng, J., Kim, T.J., Wallace, R.J.: Quantitative evaluation of machinability in abrasive waterjet machining (1992)

[24] Niranjan, C., Srinivas, S., Ramachandra, M.: Effect of process parameters on depth of penetration and topography of az91 magnesium alloy in abrasive water jet cutting. Journal of magnesium and alloys **6**(4), 366–374 (2018)

[25] Sitarama Chakravarthy, P., Ramesh Babu, N.: A new approach for selection of optimal process parameters in abrasive water jet cutting. Materials and manufacturing processes **14**(4), 581–600 (1999)

[26] Sala, S.T., Körner, R., Huber, N., Kashaev, N.: On the use of machine learning and genetic algorithm to predict the region processed by laser peen forming. Manufacturing Letters **38**, 60–64 (2023)

[27] Wu, P., He, Y., Li, Y., He, J., Liu, X., Wang, Y.: Multi-objective optimisation of machining process parameters using deep learning-based data-driven genetic algorithm and topsis. Journal of Manufacturing Systems **64**, 40–52 (2022)

[28] Jagadish, Bhowmik, S., Ray, A.: Prediction of surface roughness quality of green abrasive water jet machining: a soft computing approach. Journal of Intelligent Manufacturing **30**(8), 2965–2979 (2019)

[29] Rao, R.V., Savsani, V.J., Vakharia, D.P.: Teaching–learning-based optimization: a novel method for constrained mechanical design optimization problems. Computer-aided design **43**(3), 303–315 (2011)

[30] Cheng, M.-Y., Prayogo, D.: Symbiotic organisms search: a new metaheuristic optimization algorithm. Computers & Structures **139**, 98–112 (2014)

[31] Hoen, P.J., Bohte, S.M.: Collective intelligence with sequences of actions: Coordinating actions in multi-agent systems. In: European Conference on Machine Learning, pp. 181–192 (2003). Springer

[32] Shastri, A.S., Nargundkar, A., Kulkarni, A.J., Sharma, K.K.: Multi-cohort intelligence algorithm for solving advanced manufacturing process problems. Neural Computing and Applications **32**, 15055–15075 (2020)

[33] Kale, I.R., Pachpande, M.A., Naikwadi, S.P., Narkhede, M.N.: Optimization of advanced manufacturing processes using socio inspired cohort intelligence algorithm. International Journal for Simulation and Multidisciplinary Design Optimization **13**, 6 (2022)

[34] Korkmaz, M.E., Gupta, M.K., Çelik, E., Ross, N.S., Günay, M.: Tool wear and its mechanism in turning aluminum alloys with image processing and machine learning methods. Tribology International **191**, 109207 (2024)

[35] Zhao, W., Guo, C.: Topography and microstructure of the cutting surface machined with abrasive waterjet. The International Journal of Advanced Manufacturing Technology **73**, 941–947 (2014)

[36] Copertaro, E., Perotti, F., Castellini, P., Chiariotti, P., Martarelli, M., Annoni, M.: Focusing tube operational vibration as a means for monitoring the abrasive waterjet cutting capability. Journal of Manufacturing Processes **59**, 1–10 (2020)

[37] Kahrizi, M.: Micromachining Techniques for Fabrication of Micro and Nano Structures. BoD–Books on Demand, ??? (2012)

[38] Babu, M.K., Chetty, O.K.: A study on the use of single mesh size abrasives in abrasive waterjet machining. The International Journal of Advanced Manufacturing Technology **29**(5), 532–540 (2006)

[39] Kulkarni, A.J., Durugkar, I.P., Kumar, M.: Cohort intelligence: a self supervised learning behavior. In: 2013 IEEE International Conference on Systems, Man, and Cybernetics, pp. 1396–1400 (2013)

[40] Muther, T., Syed, F.I., Dahaghi, A.K., Negahban, S.: Socio-inspired multi-cohort intelligence and teaching-learning-based optimization for hydraulic fracturing parameters design in tight formations. Journal of Energy Resources Technology **144**(7), 073201 (2022)

[41] Kale, I.R., Sapre, M.S., Khedkar, A., Dhamankar, K., Anand, A., Singh, A.: Hybrid aco-ci algorithm for beam design problems. SN Computer Science **5**(3), 282 (2024)

[42] Mahdavi-Meymand, A., Sulisz, W., Zounemat-Kermani, M.: Hybrid and integrative evolutionary machine learning in hydrology: A systematic review and meta-analysis. Archives of Computational Methods in Engineering **31**(3), 1297–1340 (2024)

[43] Niranjan, C., Srinivas, S., Ramachandra, M.: Experimental investigations on depth of penetration and surface integrity in az91/al 2 o 3 nano-composites cut by abrasive water jet. The International Journal of Advanced Manufacturing Technology **107**, 747–762 (2020)

[44] Kashyap, K., Srinivas, S.: Effect of process parameters on depth of penetration & surface roughness in abrasive waterjet cutting of copper. Applied Mechanics and Materials **895**, 301–306 (2019)

[45] Srinivas, S., Babu, N.R.: Penetration ability of abrasive waterjets in cutting of aluminum-silicon carbide particulate metal matrix composites. Machining Science and Technology **16**(3), 337–354 (2012)

[46] Meng, J., Wei, Q., Ma, Y.: Numerical simulation study on the flow field out of a submerged abrasive water jet nozzle. Mathematical and Computational Applications **21**(1), 2 (2016)

[47] El Ghadoui, M., Mouchtachi, A., Majdoul, R.: A hybrid optimization approach

for intelligent manufacturing in plastic injection molding by using artificial neural network and genetic algorithm. Scientific Reports **13**(1), 21817 (2023)

[48] Mogul, Y.I., Mogul, I., Quadros, J.D., Mohin, M., Aabid, A., Baig, M., Malik, M.A.: Prediction of cutting depth in abrasive water jet machining of ti-6al-4v alloy using back propagation neural networks. Results in Engineering **25**, 104520 (2025)

[49] Ibrahim, S.A.B., Korkmaz, S., Cetin, M.H., Kartal, F.: Performance evaluation of the submerged abrasive water jet turning process for improving machinability of castamide. Engineering Science and Technology, an International Journal **23**(4), 801–811 (2020)

[50] Fuse, K., Vora, J., Wakchaure, K., Patel, V.K., Chaudhari, R., Saxena, K.K., Bandhu, D., Ramacharyulu, D.A.: Abrasive waterjet machining of titanium alloy using an integrated approach of taguchi-based passing vehicle search algorithm. International Journal on Interactive Design and Manufacturing (IJIDeM) **19**(3), 2249–2263 (2025)

[51] Morisset, R., Van BUI, H., COHEN, G., GREGOIRE, M., GILLES, P.: Characterization of the cutting power of the abrasive particles during titanium alloys abrasive water jet machining (2023)

[52] Thakur, P.M., Raut, D.N.: Experimental investigation on surface topography in submerged abrasive waterjet cutting of ti6al4v. Advances in Industrial and Manufacturing Engineering **6**, 100113 (2023)

[53] Abouzaid, A., Mousa, S., Ibrahim, A.M.M.: Effect of standoff distance and traverse speed on the cutting quality during the abrasive water jet machining (awjm) of brass. Machining science and technology **28**(3), 392–414 (2024)

[54] Li, X., Chen, Z., Li, X., Xu, B., Wang, S.: Experimental study on submerged nozzle damping characteristics of solid rocket motor. Aerospace **11**(9), 759 (2024)

[55] Yu, Y., Sun, T., Yuan, Y., Gao, H., Wang, X.: Experimental investigation into the effect of abrasive process parameters on the cutting performance for abrasive waterjet technology: A case study. The International Journal of Advanced Manufacturing Technology **107**, 2757–2765 (2020)

[56] Hu, J., Kang, Y., Shi, H., Wang, X., Hu, Y., Li, D.: Experimental and numerical investigation on the cavitation erosion effect and resonance effect of submerged water jets. Ships and Offshore Structures, 1–13 (2024)

[57] Kong, M., Anwar, S., Billingham, J., Axinte, D.: Mathematical modelling of abrasive waterjet footprints for arbitrarily moving jets: part i—single straight paths. International Journal of Machine Tools and Manufacture **53**(1), 58–68 (2012)

[58] Hlaváč, L.M., Gembalová, L., Štěpán, P., Hlaváčová, I.M.: Improvement of abrasive water jet machining accuracy for titanium and tinb alloy. The International Journal of Advanced Manufacturing Technology **80**, 1733–1740 (2015)

[59] Anwar, S., Axinte, D., Becker, A.: Finite element modelling of overlapping abrasive waterjet milled footprints. Wear **303**(1-2), 426–436 (2013)

[60] Billingham, J., Miron, C., Axinte, D., Kong, M.: Mathematical modelling of abrasive waterjet footprints for arbitrarily moving jets: part ii—overlapped single and multiple straight paths. International Journal of Machine Tools and Manufacture **68**, 30–39 (2013)

[61] Begic-Hajdarevic, D., Cekic, A., Mehmedovic, M., Djelmic, A.: Experimental study on surface roughness in abrasive water jet cutting. Procedia Engineering **100**, 394–399 (2015)

[62] Chithirai Pon Selvan, M., Mohana Sundara Raju, N., Sachidananda, H.: Effects of process parameters on surface roughness in abrasive waterjet cutting of aluminium. Frontiers of Mechanical Engineering **7**, 439–444 (2012)

[63] Sreekesh, K., Govindan, P.: Experimental investigation and analysis of abrasive water-jet machining process. Asian Review of Mechanical Engineering **2**(2), 42–48 (2013)

[64] Wu, L., Zou, X., Guo, Y., Fu, L.: Experimental research and parameter optimization of high-pressure abrasive water jet machining. Lubricants **13**(4), 153 (2025)

[65] Stolárik, G., Klichová, D., Poloprudskỳ, J., Chlupová, A., Nag, A., Hloch, S.: Submerged surface texturing of aisi 304l using the pulsating water jet method. Archives of Civil and Mechanical Engineering **24**(4), 207 (2024)

[66] Lima, C.E., Lebrón, R., Souza, A.J., Ferreira, N.F., Neis, P.D.: Study of influence of traverse speed and abrasive mass flowrate in abrasive water jet machining of gemstones. The International Journal of Advanced Manufacturing Technology **83**, 77–87 (2016)

[67] Hashish, M.: An investigation of milling with abrasive-waterjets (1989)

[68] Azmir, M., Ahsan, A.: Investigation on glass/epoxy composite surfaces machined by abrasive water jet machining. Journal of Materials Processing Technology **198**(1-3), 122–128 (2008)

[69] Schwartzentruber, J., Spelt, J., Papini, M.: Prediction of surface roughness in abrasive waterjet trimming of fiber reinforced polymer composites. International Journal of Machine Tools and Manufacture **122**, 1–17 (2017)